MADPH-99-1121
FERMILAB-PUB-99/221-T
hep-ph/9908236
August 1999

$e^+e^- \to t\bar{t}H$ with Non-standard Higgs Boson Couplings

T. Han[(a)], T. Huang[(b)], Z.-H. Lin[(b)], J.-X. Wang[(b)], and X. Zhang[(b,c)]

[(a)]Department of Physics, University of Wisconsin, Madison, WI 53706, USA
[(b)]Institute of High Energy Physics, Academia Sinica, Beijing, 100039, P. R. China
[(c)]Theory Group, Fermi National Accelerator Laboratory, P.O.Box 500, Batavia, IL 60510, USA

Abstract

We consider a general effective Lagrangian for couplings of a Higgs boson to the top-quark to dimension-six operators including CP violation effects. Constraints on some of them are derived from the $Z \to b\bar{b}$ data. We study the process $e^+e^- \to t\bar{t}H$ to probe the non-standard couplings. We find that at a linear collider with a c. m. energy $\sqrt{s} \sim 0.5 - 1.5$ TeV and a high luminosity of $10 - 1000$ fb^{-1}, these non-standard couplings may be sensitively probed.

1 Introduction

Given the unknown nature of electroweak symmetry breaking and the fact that the large top-quark mass is mysteriously close to the electroweak scale, $m_t \approx v/\sqrt{2}$ where $v \approx 246$ GeV is the vacuum expectation value of the Higgs field, it is very suggestive that the top-quark sector may play a significant role in the electroweak symmetry breaking [1]. If this is the case, then the next generation of collider experiments will have the potential to explore this fundamental physics associated with the Higgs and top-quark sector. At high energy e^+e^- linear colliders, a light Higgs boson as expected in the standard model (SM) and in Supersymmetric (SUSY) models will be studied in detail [2]. In connection with the top-quark sector, the most promising process to study will be the Higgs boson and top-quark associated production [3]

$$e^+e^- \to t\bar{t}H. \tag{1}$$

By scrutinizing this process in detail, one would hope to reveal the nature of the Higgs and top-quark interactions and hopefully gain some insight for physics beyond the SM.

The observability of this signal over the SM backgrounds at e^+e^- colliders has been recently considered [4]. The accuracy to determine the $t\bar{t}H$ coupling in the SM is also studied in detail [5]. Possible CP-violation effects associated with the $t\bar{t}H$ vertex have been discussed [6], in particular, in a general two-Higgs doublet model [7] and in supersymmetric models [8]. As a model-independent approach, it may be desirable to parameterize this class of physics by a low-energy effective Lagrangian with unknown couplings to be determined by experiments. Given an underlying theory, these (anomalous) couplings can be in principle calculated. Such an approach has been taken in Ref. [9] in a non-linear realization of the gauge symmetry, and in Refs. [10, 11] in a linear realization with an explicit scalar (Higgs boson) field.

In this paper, we wish to take such a model-independent approach to explore the physics in the Higgs and top-quark sector. We first introduce a linearly realized effective Lagrangian to dimension-six operators including CP violation. We classify them by power counting argument and derive constraints on some of them from $Z \to b\bar{b}$ data. We calculate their effects at the future e^+e^- linear colliders with c. m. energies $\sqrt{s} = 0.5 - 1.5$ TeV. We then study some kinematical variables for process Eq. (1) and construct

a CP asymmetry variable. We find that these non-standard couplings may be sensitively probed at high energy and high luminosity e^+e^- colliders.

2 Effective Interactions of a Higgs Boson with Top-quark

2.1 Effective Interactions

In the case of linear realization, the new physics is parameterized by higher dimensional operators which contain the SM fields and are invariant under the SM gauge group, $SU_c(3) \times SU_L(2) \times U_Y(1)$. Below the new physics scale Λ, the effective Lagrangian can be written as

$$\mathcal{L}_{eff} = \mathcal{L}_0 + \frac{1}{\Lambda^2} \sum_i C_i O_i + \mathcal{O}(\frac{1}{\Lambda^4}) \tag{2}$$

where $\mathcal{L}_0$ is the SM Lagrangian. O_i are dimension-six operators which are $SU_c(3) \times SU_L(2) \times U_Y(1)$ invariant and C_i are constants which represent the coupling strengths of O_i [10]. Recently the effective operators involving the top quark were reclassified and some are analyzed in Refs. [11, 12]. If we assume that the new physics is of the origin associated with the electroweak symmetry breaking, then it is natural to identify the cut-off scale Λ to be the order of $\mathcal{O}(4\pi v)$ and the coefficients C_i the order of unity. Alternatively, based on unitarity argument for massive quark scattering [13], the scale for new physics in the top-quark sector should be below about 3 TeV.

Following Refs. [11, 12], we find that there are seven dimension-six CP-even operators which give new contributions to the couplings of H to the top quark,

$$\begin{aligned}
O_{t1} &= (\Phi^\dagger\Phi - \frac{v^2}{2}) \left[\bar{q}_L t_R \widetilde{\Phi} + \widetilde{\Phi}^\dagger \bar{t}_R q_L\right], && (3)\\
O_{t2} &= i\left[\Phi^\dagger D_\mu \Phi - (D_\mu \Phi)^\dagger \Phi\right] \bar{t}_R \gamma^\mu t_R, && (4)\\
O_{Dt} &= (\bar{q}_L D_\mu t_R) D^\mu \widetilde{\Phi} + (D^\mu \widetilde{\Phi})^\dagger (\overline{D_\mu t_R} q_L), && (5)\\
O_{tW\Phi} &= \left[(\bar{q}_L \sigma^{\mu\nu} \tau^I t_R)\widetilde{\Phi} + \widetilde{\Phi}^\dagger (\bar{t}_R \sigma^{\mu\nu} \tau^I q_L)\right] W^I_{\mu\nu}, && (6)\\
O_{tB\Phi} &= \left[(\bar{q}_L \sigma^{\mu\nu} t_R)\widetilde{\Phi} + \widetilde{\Phi}^\dagger (\bar{t}_R \sigma^{\mu\nu} q_L)\right] B_{\mu\nu}, && (7)
\end{aligned}$$

$$O_{\Phi q}^{(1)} = i\left[\Phi^\dagger D_\mu \Phi - (D_\mu \Phi)^\dagger \Phi\right] \bar{q}_L \gamma^\mu q_L, \quad (8)$$

$$O_{\Phi q}^{(3)} = i\left[\Phi^\dagger \tau^I D_\mu \Phi - (D_\mu \Phi)^\dagger \tau^I \Phi\right] \bar{q}_L \gamma^\mu \tau^I q_L, \quad (9)$$

where Φ is the Higgs doublet with $\widetilde{\Phi} = i\sigma_2 \Phi^*$, and $\bar{q}_L = (\bar{t}_L, \bar{b}_L)$. Similarly, there are seven dimension-six CP-odd operators [14] which contribute to the couplings of H to a top quark,

$$\overline{O}_{t1} = i(\Phi^\dagger \Phi - \frac{v^2}{2})\left[\bar{q}_L t_R \widetilde{\Phi} - \widetilde{\Phi}^\dagger \bar{t}_R q_L\right], \quad (10)$$

$$\overline{O}_{t2} = \left[\Phi^\dagger D_\mu \Phi + (D_\mu \Phi)^\dagger \Phi\right] \bar{t}_R \gamma^\mu t_R, \quad (11)$$

$$\overline{O}_{Dt} = i\left[(\bar{q}_L D_\mu t_R) D^\mu \widetilde{\Phi} - (D^\mu \widetilde{\Phi})^\dagger (\overline{D_\mu t_R} q_L)\right], \quad (12)$$

$$\overline{O}_{tW\Phi} = i\left[(\bar{q}_L \sigma^{\mu\nu} \tau^I t_R)\widetilde{\Phi} - \widetilde{\Phi}^\dagger (\bar{t}_R \sigma^{\mu\nu} \tau^I q_L)\right] W^I_{\mu\nu}, \quad (13)$$

$$\overline{O}_{tB\Phi} = i\left[(\bar{q}_L \sigma^{\mu\nu} t_R)\widetilde{\Phi} - \widetilde{\Phi}^\dagger (\bar{t}_R \sigma^{\mu\nu} q_L)\right] B_{\mu\nu}, \quad (14)$$

$$\overline{O}_{\Phi q}^{(1)} = \left[\Phi^\dagger D_\mu \Phi + (D_\mu \Phi)^\dagger \Phi\right] \bar{q}_L \gamma^\mu q_L, \quad (15)$$

$$\overline{O}_{\Phi q}^{(3)} = \left[\Phi^\dagger \tau^I D_\mu \Phi + (D_\mu \Phi)^\dagger \tau^I \Phi\right] \bar{q}_L \gamma^\mu \tau^I q_L. \quad (16)$$

Operators (3)−(16) contribute to both the three-point coupling $t\bar{t}H$ as well as four-point couplings $t\bar{t}HZ$ and $t\bar{t}H\gamma$ beyond the SM. The effective Lagrangian can be viewed as a low energy (derivative) expansion. It is thus informative to examine their energy dependence and this is listed in Table 1. Operators O_{t1} and $\overline{O}_{t1}$ give the direct corrections to the top-quark Yukawa coupling and is energy-independent. Only O_{Dt} and $\overline{O}_{Dt}$ contribute to both three-point and four-point couplings and the three-point couplings are quadratically dependent on energy, due to the nature of double-derivative couplings. Explicit expressions in terms of physical states for the above operators in the unitary gauge and the corresponding Feynman rules for the vertices are presented in the Appendices.

2.2 Bounds on the Couplings

Before we move on to discuss collider phenomenology, we first examine the possible constraints on those operators from the measurement $Z \to b\bar{b}$. For an on-shell Z, one can write the effective vertex $Zb\bar{b}$ as

$$\Gamma_\mu = -i\frac{e}{4 s_W c_W}\left[\gamma_\mu V - \gamma_\mu \gamma_5 A + \frac{1}{2m_b}(p_b - p_{\bar{b}})_\mu S\right], \quad (17)$$

	$t\bar{t}H$	$t\bar{t}HZ$	$t\bar{t}H\gamma$
$O_{t1}, \overline{O}_{t1}$	1		
O_{t2}		$1/v$	
$\overline{O}_{t2}$	E/v		
$O_{Dt}, \overline{O}_{Dt}$	E^2/v^2	E/v^2	E/v^2
$O_{tW\Phi}, \overline{O}_{tW\Phi}$		E/v^2	E/v^2
$O_{tB\Phi}, \overline{O}_{tB\Phi}$		E/v^2	E/v^2
$O^{(1)}_{\Phi q}$		$1/v$	
$\overline{O}^{(1)}_{\Phi q}$	E/v		
$O^{(3)}_{\Phi q}$		$1/v$	
$\overline{O}^{(3)}_{\Phi q}$	E/v		

Table 1: The energy-dependence of dimension-six operators in Eqs. (3)-(16) for couplings $t\bar{t}H$, $t\bar{t}HZ$ and $t\bar{t}H\gamma$. An overall normalization v^2/Λ^2 has been factored out.

where $s_W = \sin\theta_W$; p_b and $p_{\bar{b}}$ are the momenta of outgoing quark and anti-quark, respectively. The vector and axial-vector couplings are written as

$$V = v_b + \delta V, \quad A = a_b + \delta A, \tag{18}$$

where v_b and a_b represent the SM couplings and δV, δA the new physics contributions. To the order of $1/\Lambda^2$, the observable R_b at the Z pole is calculated to be

$$R_b \equiv \frac{\Gamma(Z \to b\bar{b})}{\Gamma(Z \to \text{hadrons})} = R_b^{SM}\left[1 + 2\frac{v_b\delta V + a_b\delta A}{v_b^2 + a_b^2}(1 - R_b^{SM})\right], \tag{19}$$

where we have neglected the bottom quark mass. Inversely, we have

$$\delta V = \delta A = \frac{R_b^{exp} - R_b^{SM}}{(1 - R_b^{SM})R_b^{SM}}\frac{v_b^2 + a_b^2}{2(v_b + a_b)}. \tag{20}$$

The SM prediction on R_b and the latest experimental value are [15]

$$R_b^{SM} = 0.2158(2), \qquad R_b^{exp} = 0.21656(74). \tag{21}$$

If we attribute the difference as the new physics contribution, from Eq.(20) we obtain the limit at the 1σ (3σ) level

$$-3.9 \times 10^{-3}\ (-8.4 \times 10^{-3}) < \delta V < -5 \times 10^{-5}\ (3.8 \times 10^{-3}). \tag{22}$$

Operators $O_{\Phi q}^{(1)}$ and $O_{\Phi q}^{(3)}$ introduced in the last section modify the couplings at tree level. Assuming that there is no accidental cancellation between them, then they are calculated to be

$$\delta V = \delta A = -\frac{2 s_W c_W}{e} \frac{m_Z}{v} \left[\frac{v^2}{\Lambda^2} C_{\Phi q}^{(1)} + \frac{v^2}{\Lambda^2} C_{\Phi q}^{(3)} \right]. \tag{23}$$

Noting that $2 s_W c_W m_Z / ev \simeq 1$, we obtain the bound for each of them at the 1σ (3σ) level as

$$5 \times 10^{-5}\ (-3.8 \times 10^{-3}) < \frac{v^2}{\Lambda^2} C_{\Phi q}^{(1)} = \frac{v^2}{\Lambda^2} C_{\Phi q}^{(3)} < 3.9 \times 10^{-3}\ (8.4 \times 10^{-3}) \tag{24}$$

For O_{t1}, O_{t2}, O_{Dt}, $O_{tW\Phi}$ and $O_{tB\Phi}$ they are not constrained by R_b at tree level. However, at one-loop level they contribute to gauge boson self-energies, and thus rather loose bounds exist [12] with significant uncertainties. Bounds on them can also be studied from the argument of partial wave unitarity. The upper bounds are obtained in Ref. [12],

$$|C_{t1}| \simeq \frac{16\pi}{3\sqrt{2}} \left(\frac{\Lambda}{v} \right), \qquad |C_{t2}| \simeq 8\pi\sqrt{3}, \tag{25}$$

$$C_{Dt} \simeq 10.4 \ \text{ for } C_{Dt} > 0, \qquad C_{Dt} \simeq -6.4 \ \text{ for } C_{Dt} < 0, \tag{26}$$

$$|C_{tW\Phi}| \simeq 2.5, \qquad |C_{tB\Phi}| \simeq 2.5\ . \tag{27}$$

As to the new physics scale, it is plausible to envision that $\Lambda \approx 1 - 3$ TeV, but we will keep v^2/Λ^2 as a free parameter in our studies. For the convenience of our future presentation, it is informative to see the ranges of the unitarity bounds for $\Lambda \approx 3 - 1$ TeV:

$$|C_{t1}| \frac{v^2}{\Lambda^2} \simeq 1.0 - 3.0, \qquad |C_{t2}| \frac{v^2}{\Lambda^2} \simeq 0.29 - 2.6, \tag{28}$$

$$C_{Dt}\frac{v^2}{\Lambda^2} \simeq 0.07 - 0.63 \quad \text{or} \quad C_{Dt}\frac{v^2}{\Lambda^2} \simeq -(0.04 - 0.40), \tag{29}$$

$$|C_{tW\Phi}|\frac{v^2}{\Lambda^2} \simeq |C_{tB\Phi}|\frac{v^2}{\Lambda^2} \simeq 0.02 - 0.15\ . \tag{30}$$

Obviously, collider experiments have to reach a sensitivity on these couplings below this level to be useful.

Currently, there are no significant experimental constraints on the CP-odd couplings involving the top-quark sector.

3 $t\bar{t}H$ Production with Non-standard Couplings at Future e^+e^- Colliders

One would hope to explore the new interactions presented in the last section at high energy colliders. The relevant Feynman diagrams for $e^+e^- \to t\bar{t}H$ production are depicted in Fig. 1, where (a)−(c) are those in the SM and the dots denote the contribution from new interactions. We evaluate all the diagrams including interference effects, employing a helicity amplitude package developed in [16]. This package has the flexibility to include new interactions beyond the SM. We have not included the QCD corrections to the signal process, which are known to be positive and sizeable [17].

Following the power counting argument made about Table 1, we expect that modifications to the SM prediction from different operators would be distinctive at high energies. Due to the strong constraints on $O^{(1)}_{\Phi q}$ and $O^{(3)}_{\Phi q}$ from the $Z \to b\bar{b}$ measurement, the effects of these operators at colliders will be rather small. We will thus neglect them. For the purpose of illustration, we will only present results for the operators O_{t1} (energy-independent) and O_{Dt} (most sensitive to energy scale) and hope that they are representative to the others with similar energy-dependence based on the power-counting behavior. For simplicity, we assume one operator to be non-zero at a time in our study.

The production cross sections versus $\sqrt{s}$ are shown in Fig. 2, (a) for $C_{t1}v^2/\Lambda^2 = -0.16$ and (b) for $C_{Dt}v^2/\Lambda^2 = -0.40$ for $m_H = 100,\ 120$ and 140 GeV. The dashed curves are for the SM expectation. As anticipated, contributions from O_{Dt} become more significant at higher energies.

We show the Higgs boson mass dependence of the cross section in Fig. 3,

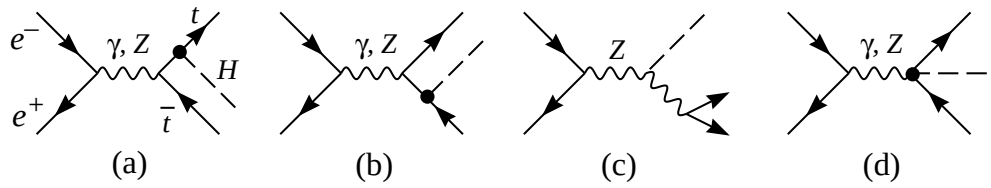

Figure 1: Feynman diagrams for $e^+e^- \to t\bar{t}H$ production. (a)-(c) are those in the SM. The dots denote the contribution from new interactions.

(a) for $\sqrt{s} = 0.5$ TeV, and (b) for $\sqrt{s} = 1$ TeV. A few representative values of the couplings C_{t1} and C_{Dt} are illustrated. The thick solid curves are for the operator O_{t1}, while the thin solid for O_{Dt}.

It is informative to study how the cross sections change versus the couplings, as shown in Fig. 4. The four panels are (a) for O_{t1} and $\sqrt{s} = 0.5$ TeV; (b) for O_{t1} and $\sqrt{s} = 1$ TeV; (c) for O_{Dt} and $\sqrt{s} = 0.5$ TeV; (d) for O_{Dt} and $\sqrt{s} = 1$ TeV with $m_H = 100,\ 120,\ 140$ GeV. Due to the interference effects, cross sections decrease as C_{t1} increases and are essentially linearly dependent upon the coupling. The effect due to the operator O_{Dt} is insignificant at $\sqrt{s} = 0.5$ TeV (Fig. 4(c)), while at higher energies the contribution from O_{Dt} is substantial and the quadratic terms become quickly important (Fig. 4(d)).

4 Sensitivity to the Non-standard Couplings

To establish the sensitivity limits on the non-standard couplings that may be probed at future linear collider experiments, one needs to consider the identification of the final state from $t\bar{t}H$, including the branching ratios and the detection efficiencies. For a light Higgs boson of current interest, its leading decay mode is $H \to b\bar{b}$. The branching ratio for this mode is about $80\% \sim 50\%$ for the mass range of $100 \sim 130$ GeV. To assure a clear signal identification, we require to identify four b-jets in the final state. We assume a 65% efficiency for single b-tagging [18]. As for the decays of $W^\pm$ from $t\bar{t}$, to effectively increase the signal rate, we include both the leptonic decay ($e^\pm, \mu^\pm$) [4] and the pure hadronic decay [5]. These amount about 85% of the $t\bar{t}$ events. With the above event selection and imposing certain selective acceptance cuts, one expects to significantly suppress the QCD and EW

background processes $e^+e^- \to gt\bar{t},\ Zt\bar{t}$ [4, 5]. We estimate an efficiency factor ϵ for detecting $e^+e^- \to t\bar{t}H$ to be

$$\epsilon = 10 - 30\%,$$

and a factor ϵ' for reducing QCD and EW background to be

$$\epsilon' = 10\%$$

in our further evaluation. The background cross sections for QCD (σ_{QCD}), electroweak (σ_{EW}) and $e^+e^- \to t\bar{t}H$ in the SM (σ_{SM}) at selective energies without branching ratios and cuts included are listed in Table 2 which are consistent with that in [5].

	σ_{SM}	σ_{EW}	σ_{QCD}
$\sqrt{s}(500\ \text{GeV})$	0.38	0.19	0.84
$\sqrt{s}(1\ \text{TeV})$	2.32	0.79	1.93
$\sqrt{s}(1.5\ \text{TeV})$	1.36	0.62	1.54

Table 2: Background cross sections σ_{SM}, σ_{EW} and σ_{QCD} in units of fb at selective energies for $m_H = 120$ GeV.

To estimate the luminosity (L) needed for probing the effects of the non-standard couplings, we define the significance of a signal rate (S) relative to a background rate (B) in terms of the Gaussian statistics,

$$\sigma_S = \frac{S}{\sqrt{B}} \tag{31}$$

for which a signal at 95% (99%) confidence level (C.L.) corresponds to $\sigma_S =$ 2 (3).

4.1 CP-even Operators

In the present of the CP-even operators, the $t\bar{t}H$ cross section (σ) would be thus modified from the SM expectation. The event rates in Eq. (31) are

calculated as

$$S = L(|\sigma - \sigma_{SM}|)\epsilon \quad \text{and} \quad B = L\left[\sigma_{SM}\epsilon + (\sigma_{QCD} + \sigma_{EW})\epsilon'\right]. \tag{32}$$

We then obtain the luminosity required for observing the effects of O_{t1} at 95% C.L. for 500 GeV and 1 TeV for C_{t1} in Fig. 5 and for 1 TeV and 1.5 TeV for C_{Dt} in Fig. 6, where the two curves are for 10% and 30% of signal detection efficiency, respectively. We see that at a 0.5 TeV collider, one would need rather high integrated luminosity to reach the sensitivity to the non-standard couplings; while at a collider with a higher c.m. energy one can sensitively probe those couplings with a few hundred fb^{-1} luminosity.

Some kinematical distributions are discriminative for the signal and backgrounds. For instance, the existence of O_{Dt} will affect the distributions of the final state particles. In Fig. 7, we plotted three distributions, $d\sigma/dE_t$, $d\sigma/dm_{t\bar{t}}$ and $d\sigma/d\cos\theta_H$. Here E_t and E_H are the energy of top quark and Higgs respectively, $m_{t\bar{t}}$ is the invariant mass of the $t\bar{t}$ system, and θ_H is the angle of Higgs with respect to the electron beam direction. Non-standard couplings typically enhance the cross section rate at higher particle energies and at the region of a central scattering angle.

4.2 CP-odd Operators

If there exist effective CP-odd operators beside the SM interaction, then CP will be violated in the Higgs and top-quark sector. Similar to the discussion in the previous section, one can try to observe the effects of the operators beyond the SM expectation. The total cross sections versus the CP-odd operators $\overline{O}_{t1}$ and $\overline{O}_{Dt}$ are shown in Fig. 8 for $m_H = 120$ GeV and $\sqrt{s} = 1$ TeV. We see that the cross sections depend on CP-odd couplings approximately quadratically. This implies that the corrections to the cross sections come from the squared terms of matrix elements and there is essentially no large interference between the SM and new operators.

To unambiguously establish the observation of CP violation, one needs to examine CP-violating observables. The CP-violating effect can be parameterized by a cross section asymmetry as

$$A_{CP} \equiv \frac{\sigma((p_1 \times p_3) \bullet p_4 < 0) - \sigma((p_1 \times p_3) \bullet p_4 > 0)}{\sigma((p_1 \times p_3) \bullet p_4 < 0) + \sigma((p_1 \times p_3) \bullet p_4 > 0)} \tag{33}$$

where p_1, p_3 and p_4 are the momenta of the incoming electron, top quark and anti-top quark, respectively. The 1σ statistical error for N_+ and N_- are $\sqrt{N}_+$ and $\sqrt{N}_-$ respectively, where N_+ is the number of the events for $(p_1 \times p_3) \bullet p_4 > 0$. and N_- is the number of the events for $(p_1 \times p_3) \bullet p_4 < 0$. Then the error for $N_+ - N_-$ is $\sqrt{(\sqrt{N}_+)^2 + (\sqrt{N}_-)^2}$. Noting that $\sqrt{(\sqrt{N}_+)^2 + (\sqrt{N}_-)^2} = \sqrt{N}$, we get the definition of the confident level for two σ as

$$\frac{N_- - N_+}{\sqrt{N}} = 2. \tag{34}$$

The asymmetry A_{CP} versus the CP-odd operators $\overline{O}_{t1}$ and $\overline{O}_{Dt}$ is shown in Fig. 9 for $m_H = 120$ GeV and $\sqrt{s} = 1$ TeV. As one can anticipate, A_{CP} depends on the couplings linearly since it comes from interference terms.

The luminosity required for detecting the effects on the total cross sections and A_{CP} is shown in Fig. 10 versus CP-odd couplings with 95% C.L for $m_H = 120$ GeV and $\sqrt{s} = 1$ TeV. The solid curves are for the cross sections with efficiency factors $\epsilon = 30\%$ and $\epsilon' = 10\%$ according to Eq. (31). The dashed curves are for A_{CP} with $\epsilon = 30\%$ according to Eq. (34). Apparently, the effects on the total cross section due to CP-odd operators are much stronger than that on A_{CP}. In other words, the direct observation of the CP asymmetry would need much higher luminosity to reach.

5 Conclusions

We have considered a general effective Lagrangian to dimension-six operators including CP violation effects. Constraints on some of the couplings can be derived from the $Z \to b\bar{b}$ data. We have studied the process $e^+e^- \to t\bar{t}H$ to explore the non-standard couplings of a Higgs boson to the top-quark. We found that future linear collider experiments should be able to probe those couplings well below their unitarity bounds. To reach good sensitivity, the integrated luminosities needed are about $\mathcal{O}(1000,\ 100,\ 10\ \text{fb}^{-1})$ for $\sqrt{s} = 0.5,\ 1.0,\ 1.5$ TeV.

Acknowledgments: We thank J.-P. Ma, Laura Reina and B.-L. Young for discussions. X. Z. would like to thank the Fermilab theory group for hospi-

tality during the final stage of this work. T. Han was supported in part by a DOE grant No. DE-FG02-95ER40896 and in part by the Wisconsin Alumni Research Foundation. T. Huang, Z.-H. Lin and X. Zhang were supported in part by the NSF of China.

Appendix A Operators

We work in the unitary gauge. The Higgs doublet can be simplified as $\Phi^\dagger = (0, H+v)/\sqrt{2}$. The expressions of the seven CP-even operators in Eqs. (3)−(9) after the electroweak symmetry breaking are given by

$$
\begin{aligned}
O_{t1} &= \frac{1}{2\sqrt{2}} H(H+2v)(H+v)(\bar{t}t), && \text{(A.1)}\\
O_{t2} &= \frac{m_Z}{v}(H+v)^2 Z^\mu(\bar{t}_R\gamma_\mu t_R), && \text{(A.2)}\\
O_{Dt} &= \frac{1}{2\sqrt{2}}\partial^\mu H\left[\partial_\mu(\bar{t}t) + \bar{t}\gamma_5\partial_\mu t - (\partial_\mu\bar{t})\gamma_5 t - i\frac{4}{3}g_1 B_\mu \bar{t}\gamma_5 t\right]\\
&\quad + i\frac{1}{2\sqrt{2}}\frac{m_Z}{v}(H+v)Z^\mu\left[\bar{t}\partial_\mu t - (\partial_\mu\bar{t})t + \partial_\mu(\bar{t}\gamma_5 t) - i\frac{4}{3}g_1 B_\mu \bar{t}t\right]\\
&\quad - i\frac{1}{2}g_2(H+v)W^-_\mu\left[\bar{b}_L\partial^\mu t_R - i\frac{2}{3}g_1 B^\mu \bar{b}_L t_R\right]\\
&\quad + i\frac{1}{2}g_2(H+v)W^+_\mu\left[(\partial^\mu\bar{t}_R)b_L + i\frac{2}{3}g_1 B^\mu \bar{t}_R b_L\right], && \text{(A.3)}\\
O_{tW\Phi} &= \frac{1}{2\sqrt{2}}(H+v)(\bar{t}\sigma^{\mu\nu}t)\left[W^3_{\mu\nu} - ig_2(W^+_\mu W^-_\nu - W^-_\mu W^+_\nu)\right]\\
&\quad + \frac{1}{2}(H+v)(\bar{b}_L\sigma^{\mu\nu}t_R)\left[W^-_{\mu\nu} - ig_2(W^-_\mu W^3_\nu - W^3_\mu W^-_\nu)\right]\\
&\quad + \frac{1}{2}(H+v)(\bar{t}_R\sigma^{\mu\nu}b_L)\left[W^+_{\mu\nu} - ig_2(W^3_\mu W^+_\nu - W^+_\mu W^3_\nu)\right], && \text{(A.4)}\\
O_{tB\Phi} &= \frac{1}{\sqrt{2}}(H+v)(\bar{t}\sigma^{\mu\nu}t)B_{\mu\nu}, && \text{(A.5)}\\
O^{(1)}_{\Phi q} &= \frac{m_Z}{v}(H+v)^2 Z_\mu\left[\bar{t}_L\gamma^\mu t_L + \bar{b}_L\gamma^\mu b_L\right], && \text{(A.6)}\\
O^{(3)}_{\Phi q} &= -\frac{m_Z}{v}(H+v)^2 Z_\mu\left[\bar{t}_L\gamma^\mu t_L - \bar{b}_L\gamma^\mu b_L\right]\\
&\quad + \frac{1}{\sqrt{2}}g_2(H+v)^2\left[W^+_\mu\bar{t}_L\gamma^\mu b_L + W^-_\mu\bar{b}_L\gamma^\mu t_L\right]. && \text{(A.7)}
\end{aligned}
$$

The expressions of the seven CP-odd operators Eqs. (10)−(16) after the electroweak symmetry breaking in the unitary gauge are given by

$$\begin{aligned}
\overline{O}_{t1} &= \frac{1}{2\sqrt{2}}H(H+2v)(H+v)(\bar{t}i\gamma_5 t), && \text{(A.8)}\\
\overline{O}_{t2} &= (H+v)\partial^\mu H(\bar{t}_R\gamma_\mu t_R), && \text{(A.9)}\\
\overline{O}_{Dt} &= i\frac{1}{2\sqrt{2}}\partial^\mu H\left[\bar{t}\partial_\mu t-(\partial_\mu\bar{t})t+\partial_\mu(\bar{t}\gamma_5 t)-i\frac{4}{3}g_1B_\mu\bar{t}t\right]\\
&\quad -\frac{1}{4\sqrt{2}}g_Z(H+v)Z^\mu\left[\partial_\mu(\bar{t}t)+\bar{t}\gamma_5\partial_\mu t-(\partial_\mu\bar{t})\gamma_5 t-i\frac{4}{3}g_1B_\mu\bar{t}\gamma_5 t\right]\\
&\quad +\frac{1}{2}g_2(H+v)W^-_\mu\left[\bar{b}_L\partial^\mu t_R-i\frac{2}{3}g_1B^\mu\bar{b}_Lt_R\right]\\
&\quad +\frac{1}{2}g_2(H+v)W^+_\mu\left[(\partial^\mu\bar{t}_R)b_L+i\frac{2}{3}g_1B^\mu\bar{t}_Rb_L\right], && \text{(A.10)}\\
\overline{O}_{tW\Phi} &= i\frac{1}{2\sqrt{2}}(H+v)(\bar{t}\sigma^{\mu\nu}\gamma_5 t)\left[W^3_{\mu\nu}-ig_2(W^+_\mu W^-_\nu-W^-_\mu W^+_\nu)\right]\\
&\quad +i\frac{1}{2}(H+v)(\bar{b}_L\sigma^{\mu\nu}t_R)\left[W^-_{\mu\nu}-ig_2(W^-_\mu W^3_\nu-W^3_\mu W^-_\nu)\right]\\
&\quad -i\frac{1}{2}(H+v)(\bar{t}_R\sigma^{\mu\nu}b_L)\left[W^+_{\mu\nu}-ig_2(W^3_\mu W^+_\nu-W^+_\mu W^3_\nu)\right], && \text{(A.11)}\\
\overline{O}_{tB\Phi} &= i\frac{1}{\sqrt{2}}(H+v)(\bar{t}\sigma^{\mu\nu}\gamma_5 t)B_{\mu\nu}, && \text{(A.12)}\\
\overline{O}^{(1)}_{\Phi q} &= (H+v)\partial_\mu H\left[\bar{t}_L\gamma^\mu t_L+\bar{b}_L\gamma^\mu b_L\right], && \text{(A.13)}\\
\overline{O}^{(3)}_{\Phi q} &= -\overline{O}^{(1)}_{\Phi q}+2(H+v)\partial_\mu H\bar{b}_L\gamma^\mu b_L\\
&\quad -\frac{i}{\sqrt{2}}g_2(H+v)^2(W^+_\mu\bar{t}_L\gamma^\mu b_L-W^-_\mu\bar{b}_L\gamma^\mu t_L), && \text{(A.14)}
\end{aligned}$$

where g_1 and g_2 are the gauge couplings for $U(1)$ and $SU(2)$, $g_Z = 2m_Z/v = \sqrt{g_1^2+g_2^2}$.

Appendix B Vertices

The momentum for a fermion is in the direction of a fermion line. The momentum for a boson is incoming into the vertex. That is, for $\bar{t}(p_1) - t(p_2) - h(p_3)$, p_2 and p_3 are incoming and p_1 is outgoing; for $Z^0_\mu(p_4) - h(p_1) - t(p_3) - \bar{t}(p_2)$ or $\gamma_\mu(p_4) - h(p_1) - t(p_3) - \bar{t}(p_2)$, p_4, p_1, p_3 are incoming and p_2

is outgoing. $P_{L,R}$ below are defined as $(1 \mp \gamma_5)/2$.

CP-even Vertices

$$\overline{t}(p_1) - t(p_2) - h(p_3): \qquad i\frac{v^2}{\sqrt{2}}\frac{C_{t1}}{\Lambda^2}$$

$$Z^0{}_\mu(p_4) - h(p_1) - t(p_3) - \overline{t}(p_2): \qquad im_Z\frac{C_{t2}}{\Lambda^2}(\gamma_5\gamma_\mu - \gamma_\mu)$$

$$\overline{t}(p_1) - t(p_2) - h(p_3): \qquad i\frac{1}{2\sqrt{2}}\frac{C_{Dt}}{\Lambda^2}(-p_1\cdot p_3 + p_2\cdot p_3 + \gamma_5 p_1\cdot p_3 + \gamma_5 p_2\cdot p_3)$$

$$Z^0{}_\mu(p_4) - h(p_1) - t(p_3) - \overline{t}(p_2): \qquad i\frac{g_2}{12\sqrt{2}c_W}\frac{C_{Dt}}{\Lambda^2}\times$$
$$(-3p_{2\mu} - 3p_{3\mu} - 8\gamma_5 p_{1\mu}s_W^2 + 3\gamma_5 p_{2\mu} - 3\gamma_5 p_{3\mu})$$

$$\gamma_\mu(p_4) - h(p_1) - t(p_3) - \overline{t}(p_2): \qquad i\frac{\sqrt{2}}{3}g_2 s_W\frac{C_{Dt}}{\Lambda^2}\gamma_5 p_{1\mu}$$

$$Z^0{}_\mu(p_4) - h(p_1) - t(p_3) - \overline{t}(p_2): \qquad \frac{c_W}{2\sqrt{2}}\frac{C_{tW\Phi}}{\Lambda^2}\sigma_{\mu\nu}p_4^\nu$$

$$\gamma_\mu(p_4) - h(p_1) - t(p_3) - \overline{t}(p_2): \qquad \frac{s_W}{2\sqrt{2}}\frac{C_{tW\Phi}}{\Lambda^2}\sigma_{\mu\nu}p_4^\nu$$

$$Z^0{}_\mu(p_4) - h(p_1) - t(p_3) - \overline{t}(p_2): \qquad -\frac{s_W}{2\sqrt{2}}\frac{C_{tB\Phi}}{\Lambda^2}\sigma_{\mu\nu}p_4^\nu$$

$$\gamma_\mu(p_4) - h(p_1) - t(p_3) - \overline{t}(p_2): \qquad \frac{c_W}{2\sqrt{2}}\frac{C_{tB\Phi}}{\Lambda^2}\sigma_{\mu\nu}p_4^\nu$$

$$Z^0{}_\mu(p_4) - h(p_1) - t(p_3) - \overline{t}(p_2): \qquad -i2m_Z\frac{C^{(1)}_{\Phi q}}{\Lambda^2}\gamma_\mu P_L$$

$$Z^0{}_\mu(p_4) - h(p_1) - t(p_3) - \overline{t}(p_2): \qquad i2m_Z\frac{C^{(3)}_{\Phi q}}{\Lambda^2}\gamma_\mu P_L$$

CP-odd Vertices

$$\overline{t}(p_1) - t(p_2) - h(p_3): \qquad i\frac{v^2}{\sqrt{2}}\frac{\overline{C}_{t1}}{\Lambda^2}(i\gamma^5)$$

$$\overline{t}(p_1) - t(p_2) - h(p_3): \qquad -v\frac{\overline{C}_{t2}}{\Lambda^2}\gamma_\mu P_R p_3^\mu$$

$$\overline{t}(p_1) - t(p_2) - h(p_3): \qquad \frac{1}{2\sqrt{2}}\frac{\overline{C}_{Dt}}{\Lambda^2}(-p_1\cdot p_3 - p_2\cdot p_3 + \gamma_5 p_1\cdot p_3 - \gamma_5 p_2\cdot p_3)$$

$$Z^0{}_\mu(p_4) - h(p_1) - t(p_3) - \overline{t}(p_2): \qquad \frac{g_2}{12\sqrt{2}c_W}\frac{\overline{C}_{Dt}}{\Lambda^2}\times$$
$$(8s_W^2 p_{1\mu} - 3p_{2\mu} + 3p_{3\mu} + 3\gamma_5 p_{2\mu} + 3\gamma_5 p_{3\mu})$$

$$\gamma_\mu(p_4) - h(p_1) - t(p_3) - \overline{t}(p_2): \qquad -\frac{\sqrt{2}}{3}g_2\sin\theta_w\frac{\overline{C}_{Dt}}{\Lambda^2}p_{1\mu}$$

$$Z^0{}_\mu(p_4) - h(p_1) - t(p_3) - \overline{t}(p_2): \qquad \frac{\cos\theta_w}{2\sqrt{2}}\frac{\overline{C}_{tW\Phi}}{\Lambda^2}(i\gamma^5)\sigma_{\mu\nu}p_4^\nu$$

$$\gamma_\mu(p_4) - h(p_1) - t(p_3) - \overline{t}(p_2): \qquad \frac{\sin\theta_w}{2\sqrt{2}}\frac{\overline{C}_{tW\Phi}}{\Lambda^2}(i\gamma^5)\sigma_{\mu\nu}p_4^\nu$$

$$Z^0{}_\mu(p_4) - h(p_1) - t(p_3) - \overline{t}(p_2): \qquad -\frac{\sin\theta_w}{2\sqrt{2}}\frac{\overline{C}_{tB\Phi}}{\Lambda^2}(i\gamma^5)\sigma_{\mu\nu}p_4^\nu$$

$$\gamma_\mu(p_4) - h(p_1) - t(p_3) - \overline{t}(p_2): \qquad \frac{\cos\theta_w}{2\sqrt{2}}\frac{\overline{C}_{tB\Phi}}{\Lambda^2}(i\gamma^5)\sigma_{\mu\nu}p_4^\nu$$

$$\overline{t}(p_1) - t(p_2) - h(p_3): \qquad -\frac{\overline{C}^{(1)}_{\Phi q}}{\Lambda^2}v\gamma_\mu P_L p_3^\mu$$

$$\overline{t}(p_1) - t(p_2) - h(p_3): \qquad \frac{\overline{C}^{(3)}_{\Phi q}}{\Lambda^2}v\gamma_\mu P_L p_3^\mu$$

References

[1] Bardeen, Hill and Lindner, Phys. Rev. **D41**, 1647 (1990); C. T. Hill, Phys. Lett. **B266**, 419 (1991); B. A. Dobrescu and C. T. Hill, Phys. Rev. Lett. **81**, 2634 (1998); R. S. Chivukula, B. A. Dobrescu, H. Georgi, C. T. Hill, Phys. Rev. **D59**, 075003 (1999).

[2] For a recent review on the Higgs boson searches at linear colliders, see *e.g.*, M. Carena, P. Zerwas, E. Gross and P. Janot, CERN-TH-95-151 (hep-ph/9602250).

[3] K.J.F. Gaemers and G.J. Gounaris, Phys. Lett. **B77**, 379 (1978); A. Djouadi, J. Kalinowski and P. Zerwas, Z. Phys. **C54**, 255 (1992).

[4] S. Moretti, Phys. Lett. **B452**, 338 (1999).

[5] H. Baer, S. Dawson and L. Reina, hep-ph/9906419.

[6] D. Chang and W.-Y. Keung, Phys. Rev. **D48**, 3225 (1993); J. Gunion, B. Grzadkowski and X.-G. He, Phys. Rev. Lett.**77**, 5172 (1996).

[7] B. Grzadkowski, J. F. Gunion and J. Kalinowski, hep-ph/9902308.

[8] A. Pilaftsis, Nucl. Phys. **B504**, 61 (1997); A. Pilaftsis, Phys. Lett. **B435**, 88 (1998); K.S. Babu, C. Kolda, J. March-Russell and Frank Wilczek, Phys. Rev. **D59**, 016004 (1999); A. Pilaftsis and C. E. M. Wagner, hep-ph/9902371.

[9] R.D. Peccei and X. Zhang, Nucl. Phys. **B337**, 269 (1990); R.D. Peccei, S. Peris and X. Zhang, Nucl. Phys. **B349**, 305 (1991).

[10] C. J. C. Burgess and H. J. Schnitzer, Nucl. Phys. **B228**, 454 (1983); C. N. Leung, S. T. Love and S. Rao, Z. Phys. **C31**, 433 (1986); W. Buchmuller and D. Wyler, Nucl. Phys. **B268**, 621 (1986); K. Hagiwara, S. Ishihara, R. Szalapski and D. Zeppenfeld, Phys. Rev. **D48**, 2182 (1993).

[11] K. Whisnant, J. M. Yang, B.-L. Young and X. Zhang, Phys. Rev. **D56**, 467 (1997).

[12] G. J. Gounaris, D. T. Papadamou, F. M. Renard, Z. Phys. **C76**, 333 (1997).

[13] M. Chanowitz, M. Furman and I. Hinchliffe, Nucl. Phys. **B153**, 402 (1979); T. Appelquist and M. Chanowitz, Phys. Rev. Lett. **59**, 2405 (1987); S. Jager and S. Willenbrock, Phys. Lett. **B435**, 139 (1998); R. S. Chivukula, Phys. Lett. **B439**, 389 (1998).

[14] J. M. Yang and B.-L Young, Phys. Rev. **D56**, 5907 (1997).

[15] J. Erler and P. Langacker, hep-ph/9809352.

[16] J.-X Wang, Computer Phys. Commun. 86 (1993) 214-231; J.-X. Wang, preprint KEK-TH-412 (1993), also in the Proceedings of AI93, Oberamergau, Germany; J.-X. Wang, in the Proceedings of AI96, Sept. 1996, Lausane, Switzerland.

[17] S. Dawson and L. Reina, Phys. Rev. **D57**, 5851 (1998); Phys. Rev. **D59**, 054012 (1999); S. Dittmaier, M. Kramer, Y. Liao, M. Spira, P. M. Zerwas, Phys. Lett. **B441**, 383 (1998).

[18] C. Damerall and D. Jackson, p.442, in the Proceedings of *the 1996 DPF/DPB Summer Study on High-Energy Physics*, Snowmass, Colorado.

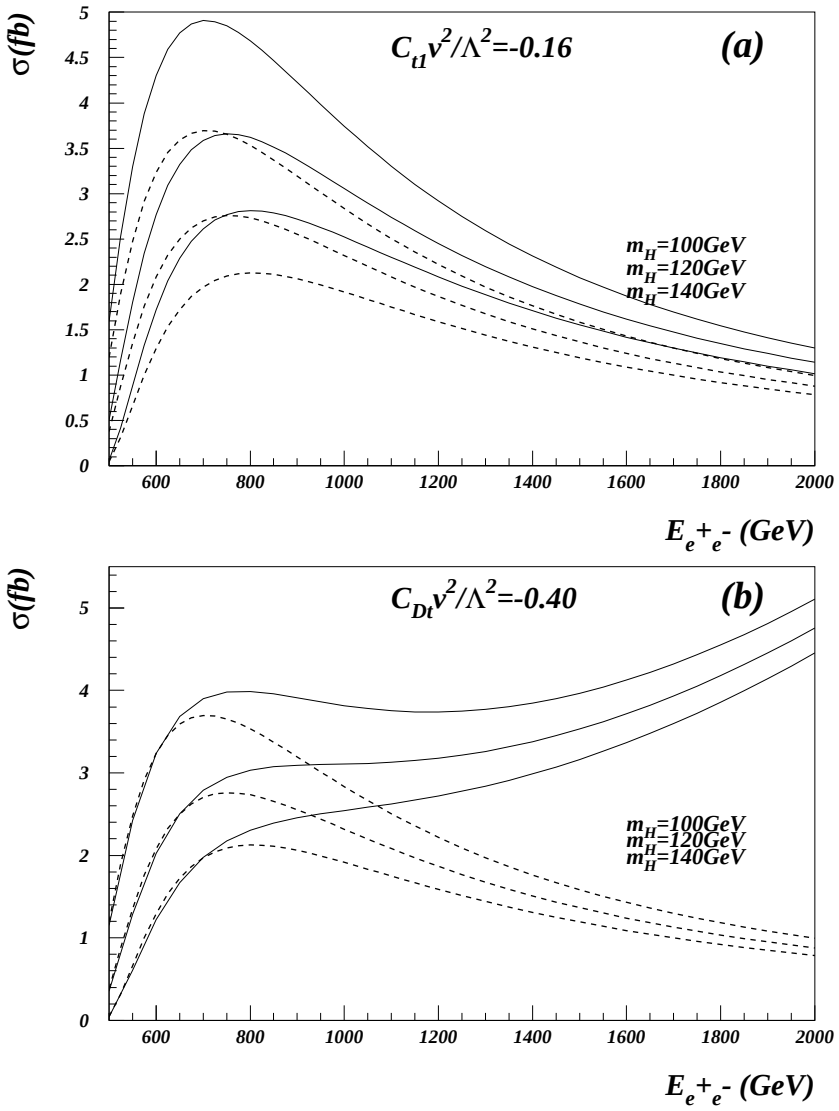

Figure 2: Total cross section for $e^+e^- \to t\bar{t}H$ production versus the e^+e^- c. m. energy for m_H = 100, 120 and 140 GeV, with (a) for O_{t1} and (b) for O_{Dt}. The dashed curves are for the SM expectation.

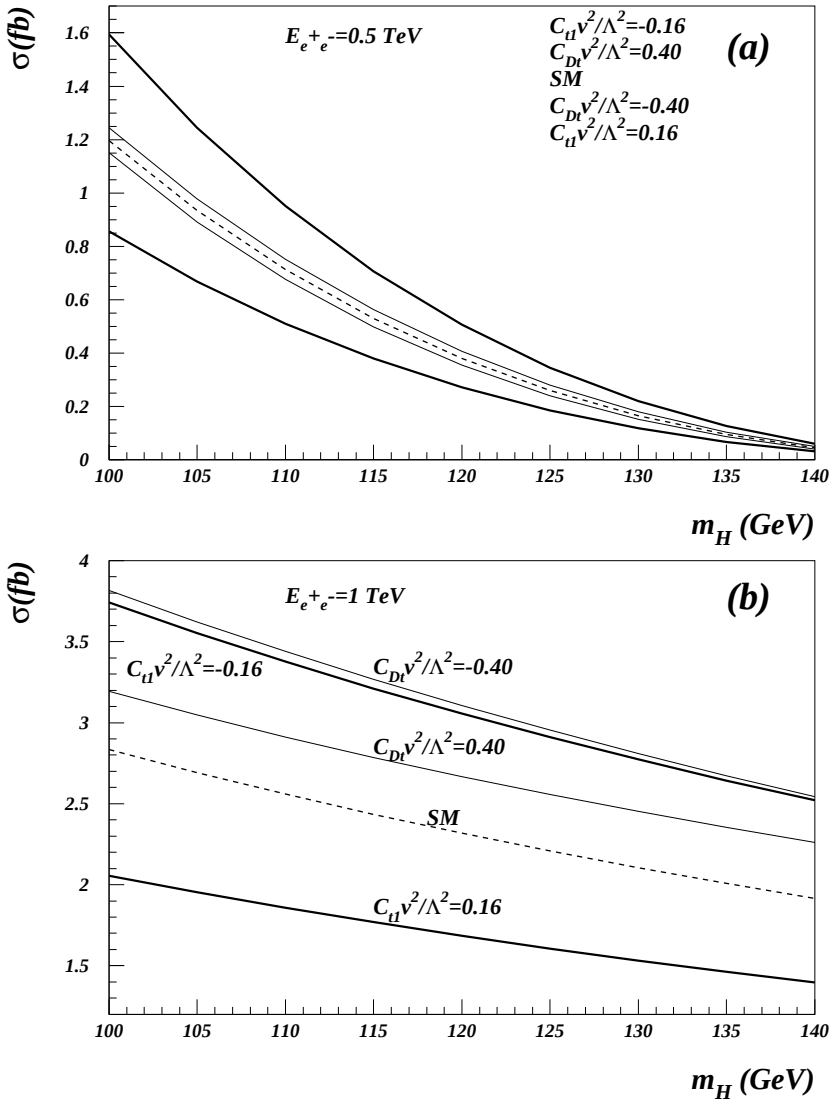

Figure 3: Total cross section for $e^+e^- \to t\bar{t}H$ production versus m_H (a) for $\sqrt{s} = 0.5$ TeV and (b) for $\sqrt{s} = 1$ TeV. The dashed curves are for the SM expectation.

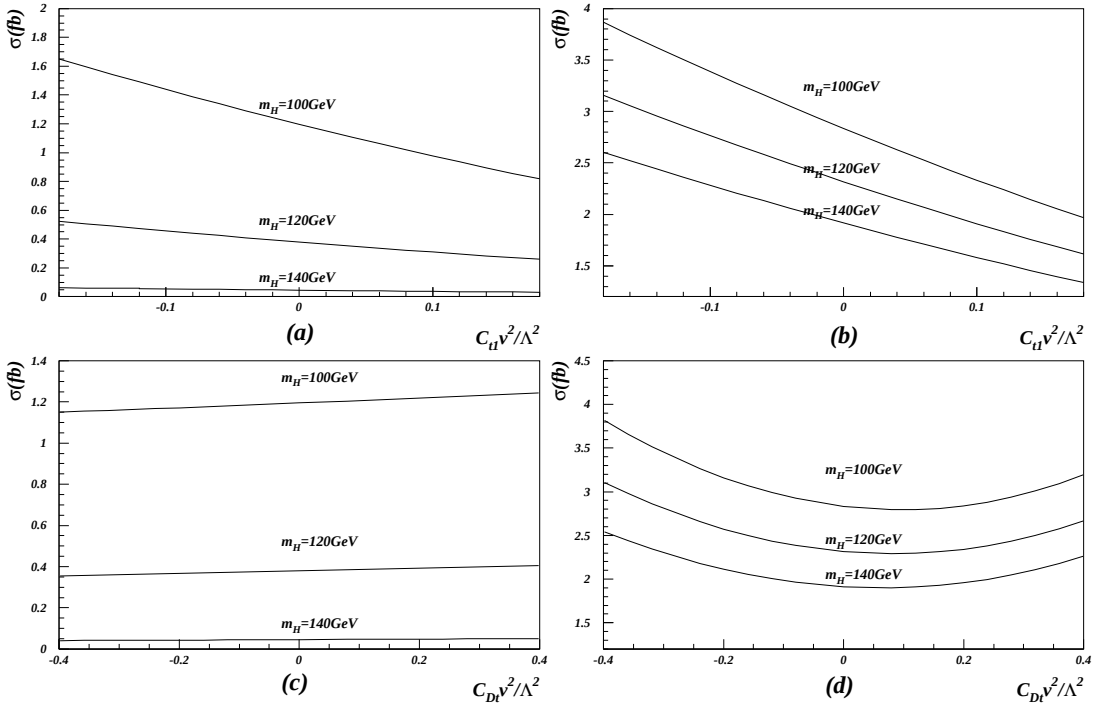

Figure 4: Total cross section for $e^+e^- \to t\bar{t}H$ production versus the couplings (a) for O_{t1} and $\sqrt{s} = 0.5$ TeV ; (b) for O_{t1} and $\sqrt{s} = 1$ TeV ; (c) for O_{Dt} and $\sqrt{s} = 0.5$ TeV ; (d) for O_{Dt} and $\sqrt{s} = 1$ TeV with $m_H = 100,\ 120,\ 140$ GeV.

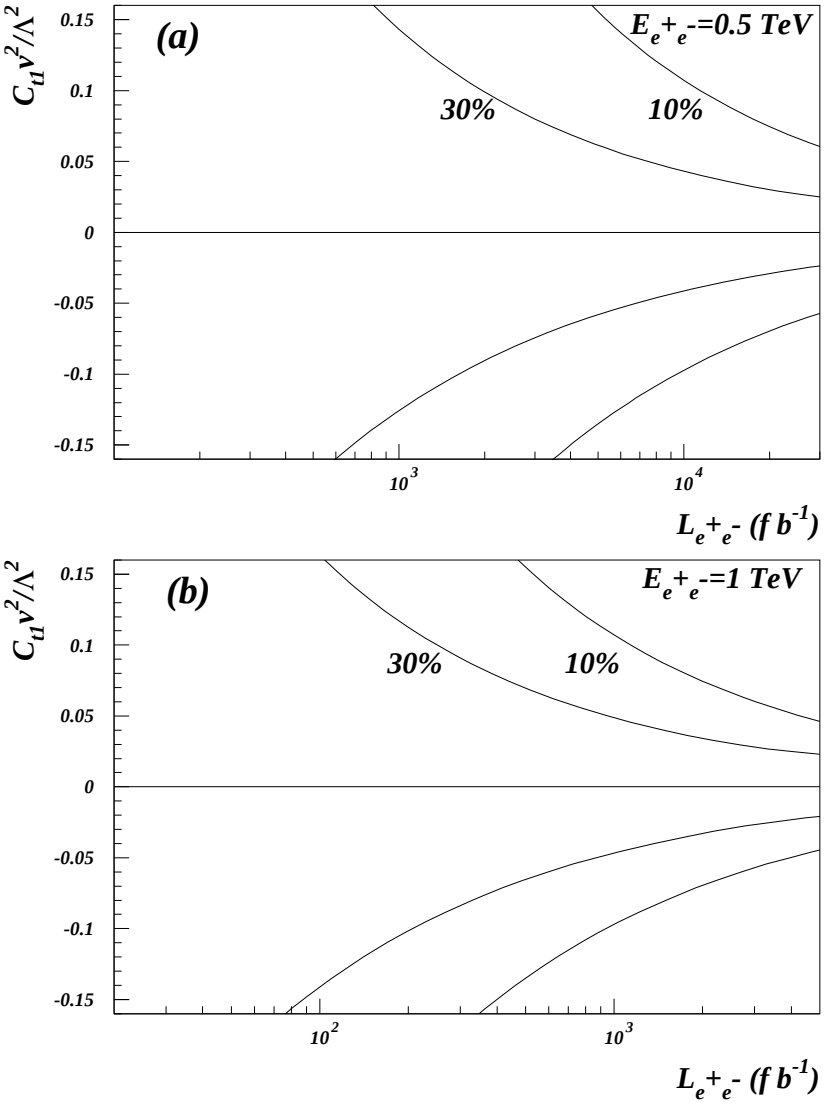

Figure 5: Sensitivity to the anomalous couplings O_{t1} versus the integrated luminosity for a 95% confidence level limits at (a) $\sqrt{s} = 0.5$ TeV and (b) $\sqrt{s} = 1$ TeV, with $m_H = 120\ GeV$.

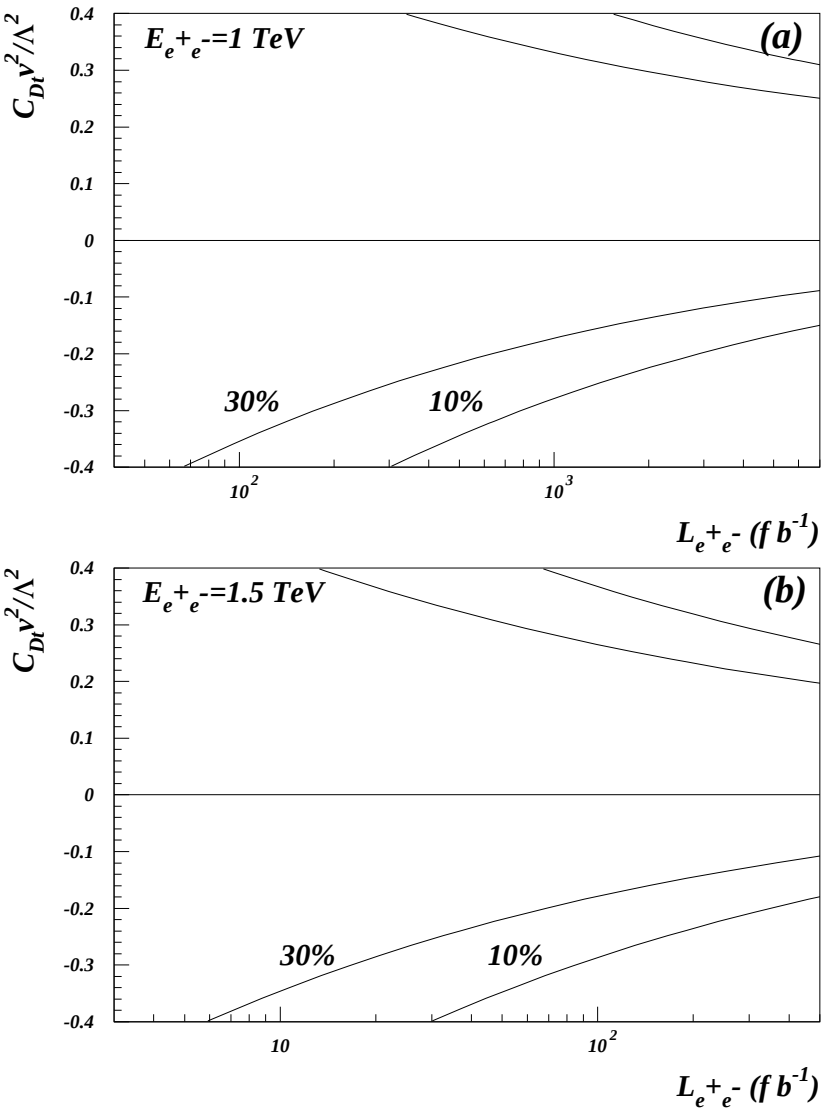

Figure 6: Sensitivity to the anomalous couplings O_{Dt} versus the integrated luminosity for a 95% confidence level limits at (a) $\sqrt{s} = 1$ TeV and (b) $\sqrt{s} = 1.5$ TeV, with $m_H = 120\ GeV$.

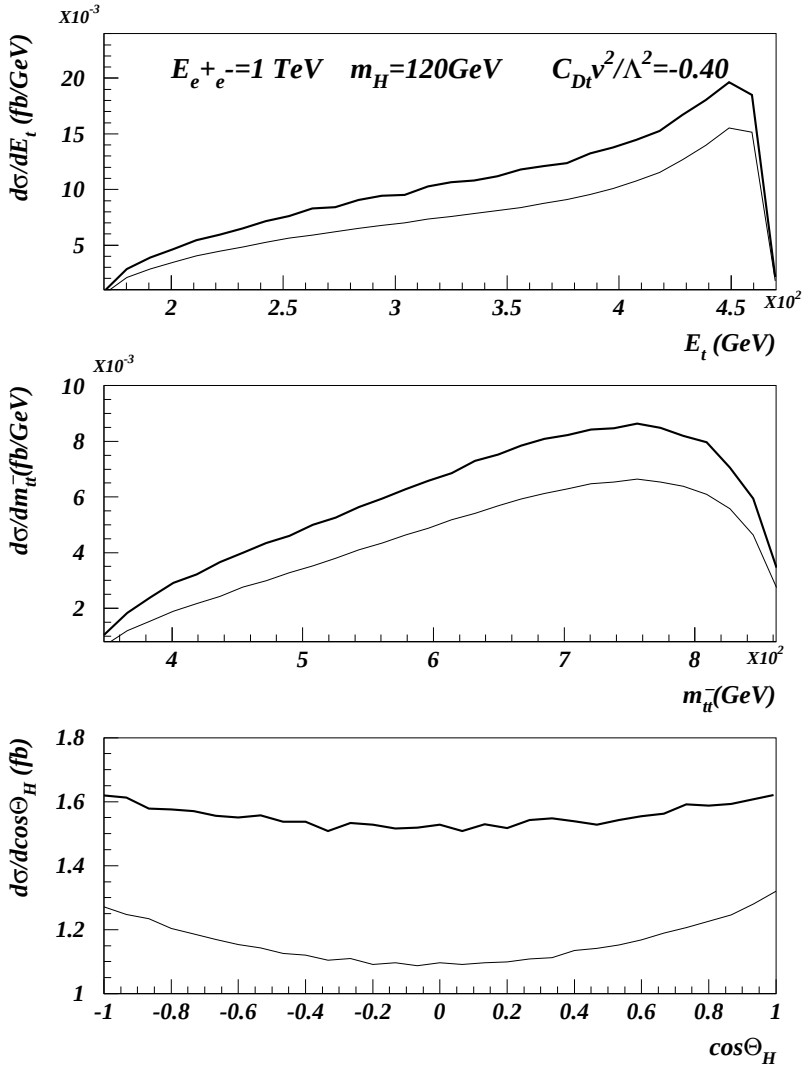

Figure 7: Kinematical distributions for $d\sigma/dE_t$, $d\sigma/dm_{tt}$, and $d\sigma/d\cos\theta_H$ with $m_H = 120$ GeV, $C_{Dt}v^2/\Lambda^2 = -0.40$ and for $\sqrt{s} = 1$ TeV.

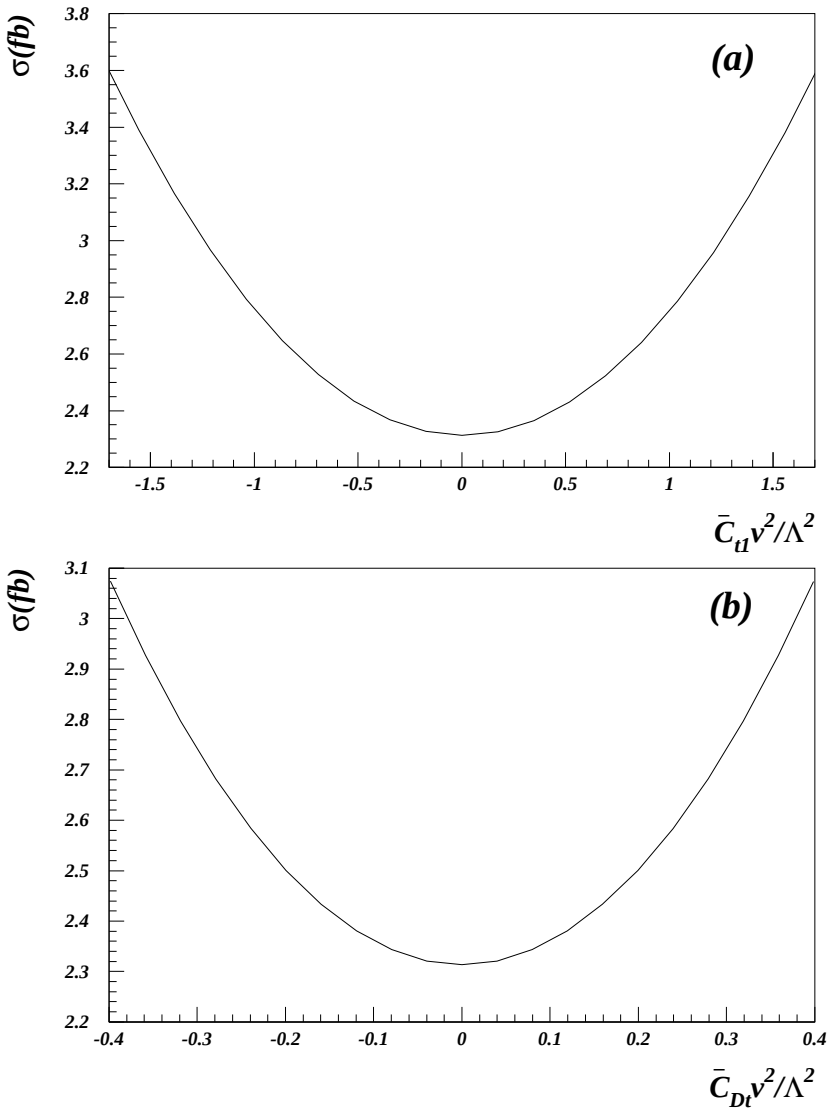

Figure 8: The total cross section versus CP-odd couplings for $m_H = 120$ GeV, $\sqrt{s} = 1$ TeV.

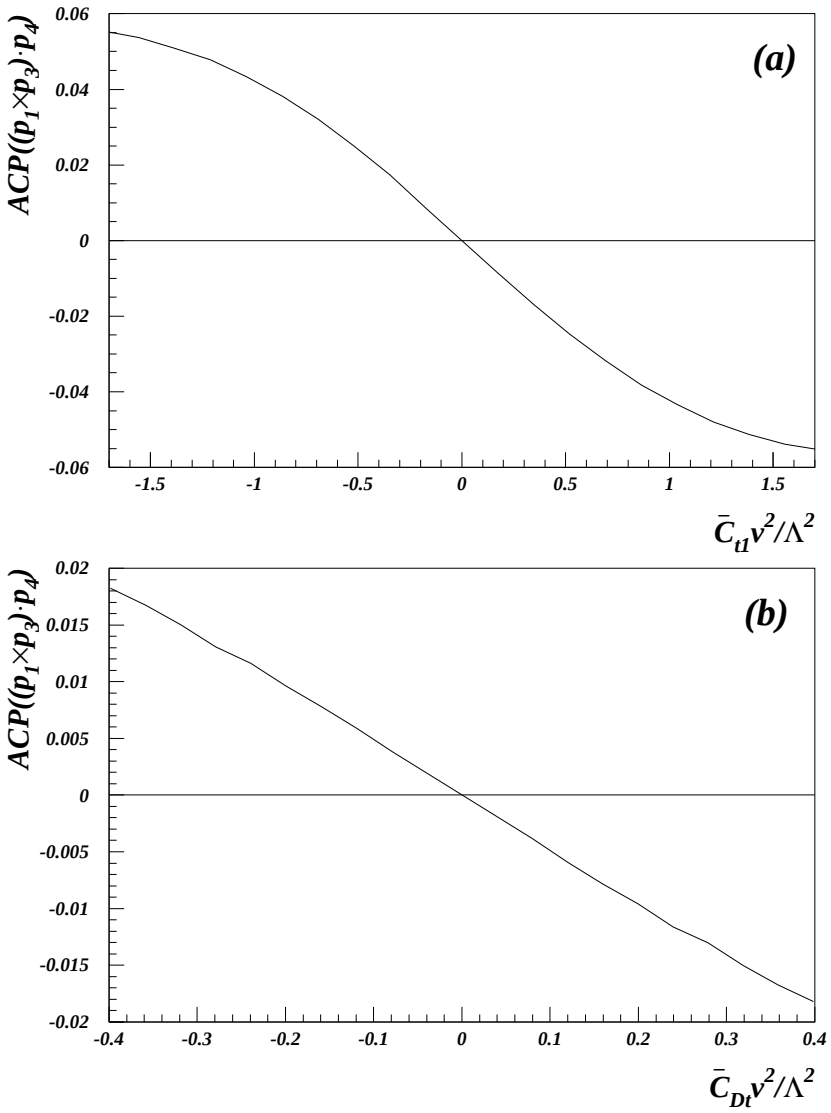

Figure 9: The CP asymmetry A_{CP} versus CP-odd couplings for $m_H = 120$ GeV, $\sqrt{s} = 1$ TeV.

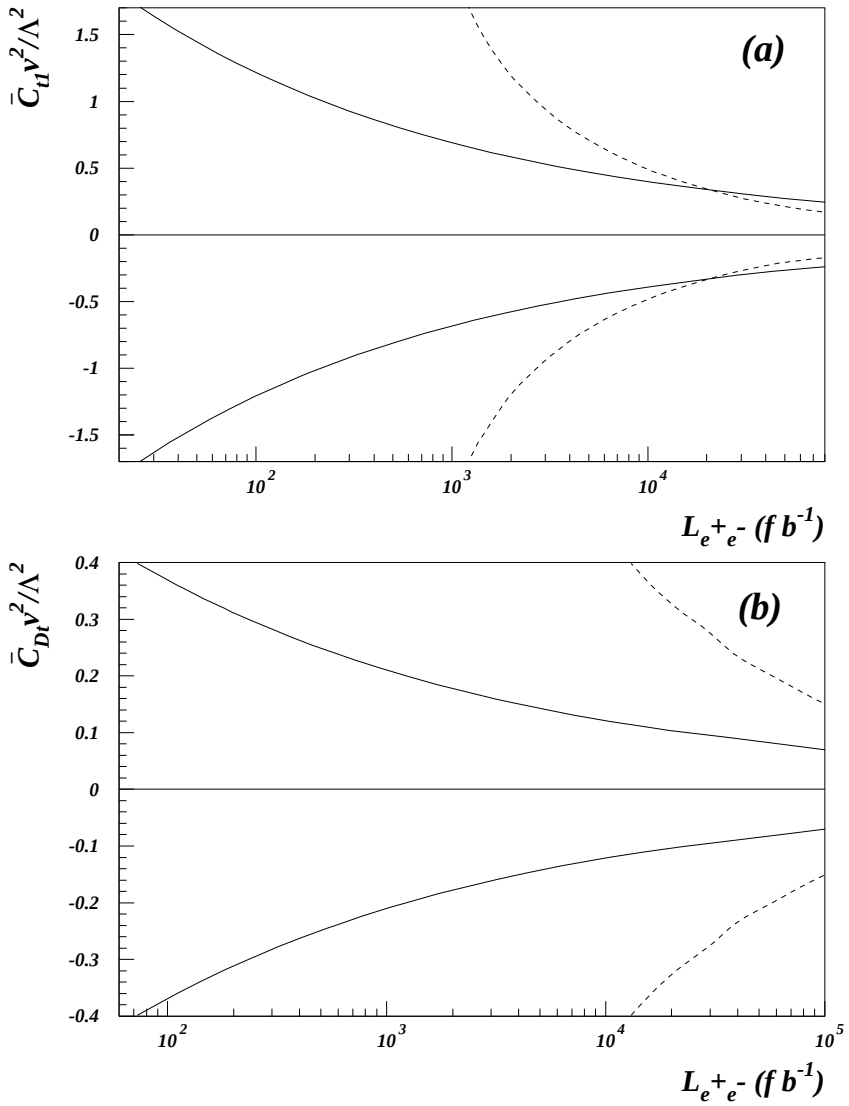

Figure 10: Sensitivity to the anomalous CP-odd couplings versus the integrated luminosity for a 95% confidence level limits and for 30% of detection efficiency at $\sqrt{s} = 1$ TeV , with $m_H = 120$ GeV. The solid line is for the total cross section and the dash line is for the CP asymmetry A_{CP}.